

## Supporting Information

### **Fabrication of defect-rich MoS<sub>2</sub> ultrathin nanosheets for application in lithium-ion batteries and supercapacitors**

Zhengcui Wu,\* Baoer Li, Yejing Xue, Jingjing Li, Yali Zhang and Feng Gao\*

Anhui Key Laboratory of Molecule-Based Materials, The Key Laboratory of Functional Molecular Solids, Ministry of Education, College of Chemistry and Materials Science, Anhui Normal University, Wuhu 241000, P. R. China.

\*Corresponding author. E-mail: zhengcui@mail.ahnu.edu.cn; fgao@mail.ahnu.edu.cn.

Tel.: +86 553 3869302; Fax: +86 553 3869302.

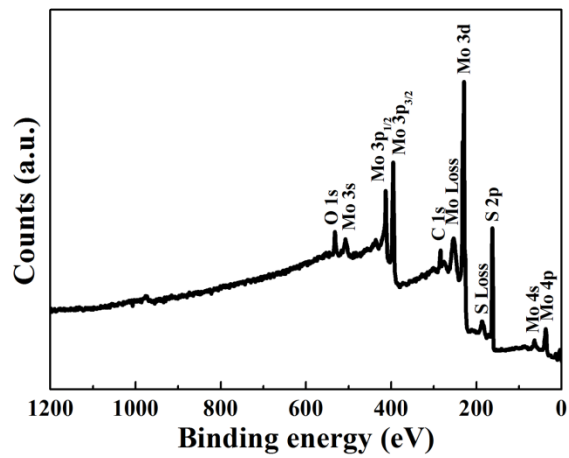


**Fig. S1** Survey XPS spectrum of the defect-rich MoS<sub>2</sub> ultrathin nanosheets.

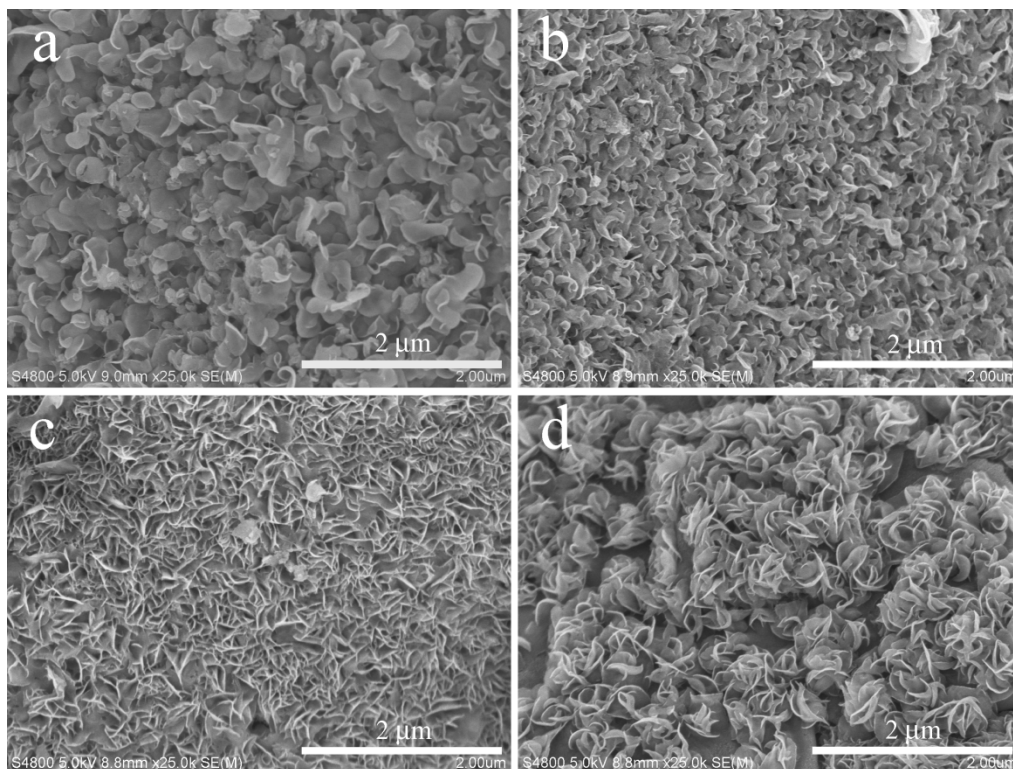


**Fig. S2** FESEM images of MoS<sub>2</sub> nanostructures synthesized under different concentrations of L-cysteine and 1, 6-hexanediamine. (a) with L-cysteine halved; (b) with L-cysteine doubled; (c) with 1, 6-hexanediamine decreased to 15 mL; and (d) with 1, 6-hexanediamine increased to 22.5 mL.

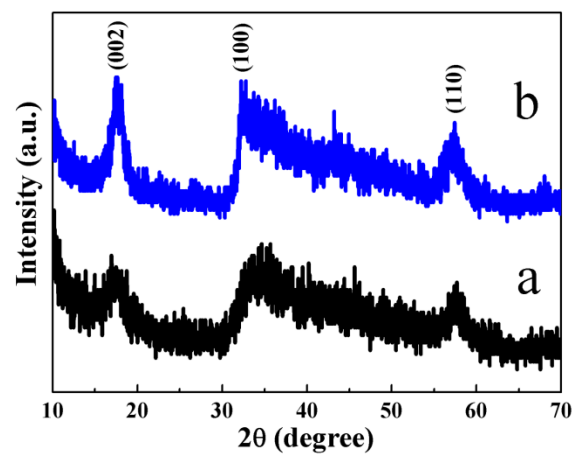


**Fig. S3** XRD patterns of the MoS<sub>2</sub> flowers (a) and chains (b).

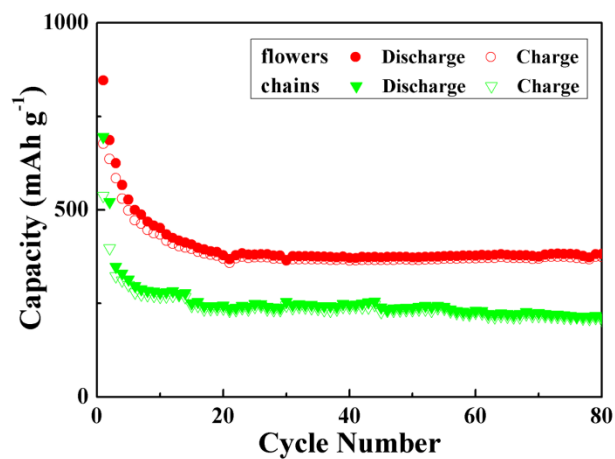


**Fig. S4** Cycling behaviors of the MoS<sub>2</sub> flowers and chains electrodes at a current density of 100 mA g<sup>-1</sup> in lithium-ion batteries.

The initial discharge capacity of the MoS<sub>2</sub> flowers is 847 mAh g<sup>-1</sup>, and the reversible discharge capacity is 382 mAh g<sup>-1</sup> after 80 cycles, which is 45.1% of the initial capacity. Meanwhile, the initial discharge capacity of the MoS<sub>2</sub> chains is 695 mAh g<sup>-1</sup>, and the reversible discharge capacity is 212 mAh g<sup>-1</sup> after 80 cycles, which is 30.5% of the initial capacity.

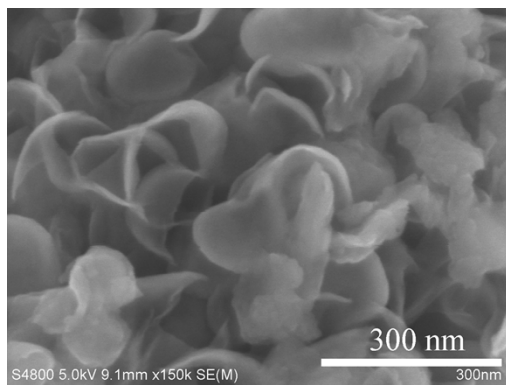


**Fig. S5** The FESEM image of the defect-rich MoS<sub>2</sub> ultrathin nanosheets after 80 charge/discharge cycles in lithium-ion battery.

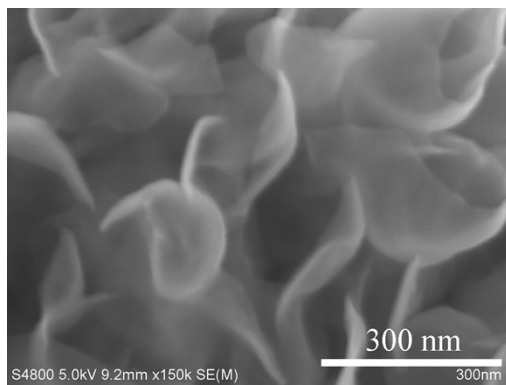


**Fig. S6** The FESEM image of the defect-rich MoS<sub>2</sub> ultrathin nanosheets after 2000 charge/discharge cycles in supercapacitor.

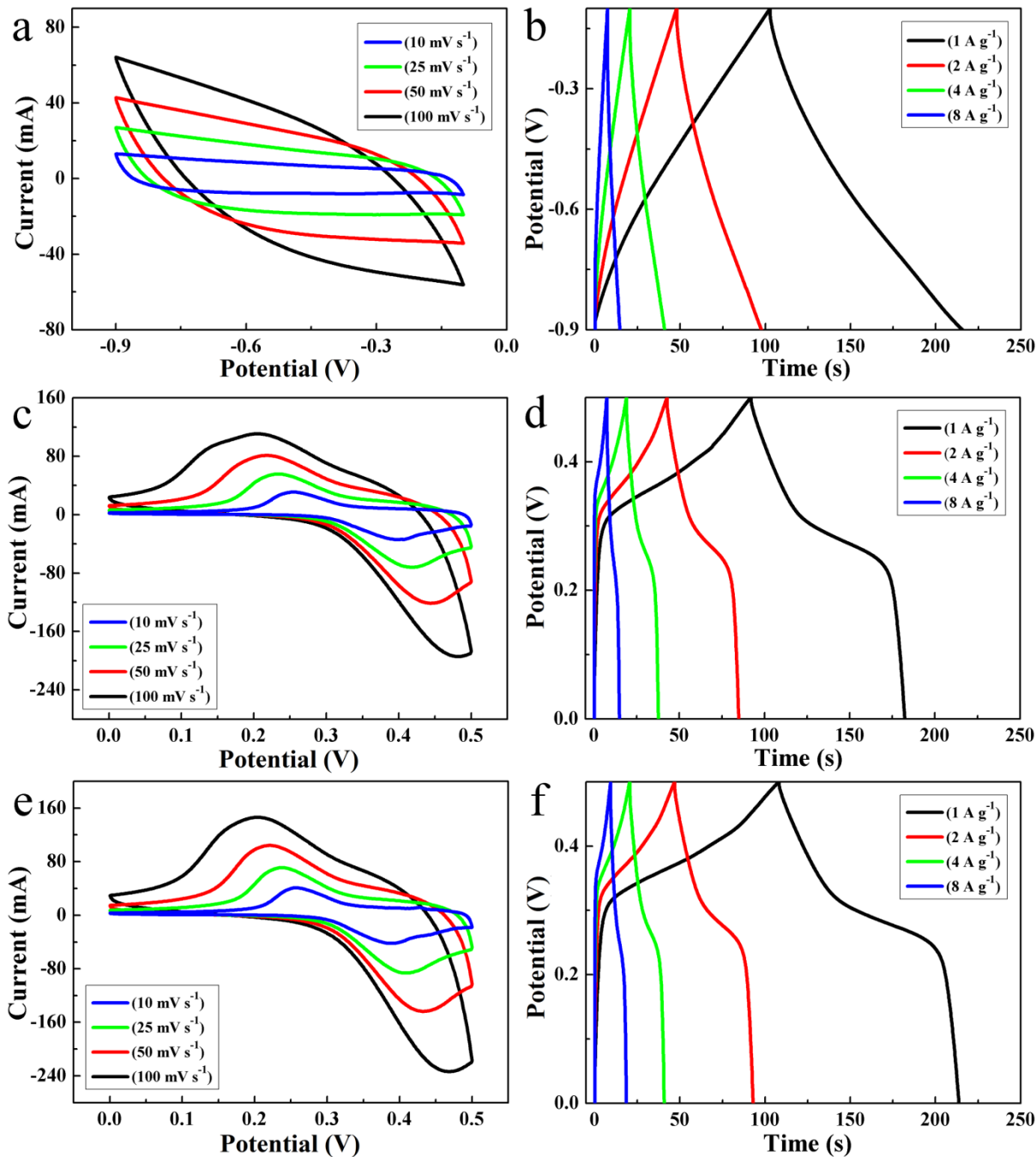


**Fig. S7** The supercapacitor performances of the defect-rich MoS<sub>2</sub> ultrathin nanosheets electrodes with the electrolytes of Na<sub>2</sub>SO<sub>4</sub>, LiOH and KOH. (a, c, e) CVs at different scans with Na<sub>2</sub>SO<sub>4</sub>, LiOH and KOH solution, respectively; and (b, d, f) Galvanostatic charge/discharge curves at different current densities with Na<sub>2</sub>SO<sub>4</sub>, LiOH and KOH solution, respectively.



The CV curves of the defect-rich MoS<sub>2</sub> ultrathin nanosheets electrode measured at different scan rates of 10, 25, 50 and 100 mV s<sup>-1</sup> in 1 M Na<sub>2</sub>SO<sub>4</sub> exhibit no obvious redox peaks (Fig. S7a), indicating typical double-layer capacitance, which are similar with those in KCl solution. The specific capacitances of the electrode calculated from the CV curves are 196.3, 160.7, 117.5 and 72.7 F g<sup>-1</sup> at scan rates of 10, 25, 50 and 100 mV s<sup>-1</sup>, respectively. The specific capacitance of our defect-rich MoS<sub>2</sub> ultrathin nanosheets electrode is larger than that of the pure MoS<sub>2</sub> nanosheets electrode with 156 F g<sup>-1</sup> at a scan rate of 20 mV s<sup>-1</sup>.<sup>1</sup> Galvanostatic charge/discharge curves of the MoS<sub>2</sub> electrode recorded at various current densities exhibit close to ideal triangular capacitive behavior (Fig. S7b). The specific capacitances calculated are 141.1, 124.5, 102.5 and 73.0 F g<sup>-1</sup> at the current densities of 1, 2, 4 and 8 A g<sup>-1</sup>, respectively. A decrease in capacitance at higher scan rate and current density is due to the lower diffusion of the charged ions.<sup>2</sup> The specific capacitance of our MoS<sub>2</sub> electrode is larger than that of the MoS<sub>2</sub> nanosheets electrode with 129.2 F g<sup>-1</sup> at current density of 1 A g<sup>-1</sup>.<sup>3</sup>

The CV curves of the defect-rich MoS<sub>2</sub> ultrathin nanosheets electrode in 3 M LiOH solution measured at different scan rates of 10, 25, 50 and 100 mV s<sup>-1</sup> between 0 and 0.5 V exhibit remarkable reversible redox peaks (Fig. S7c), suggesting the pseudocapacitive properties of the electrode. It is also observed that the redox peaks are gradually expanded and distorted with increased scan rate. The specific capacitances of the electrode calculated from the CV curves show the capacitance is 308.7, 263.7, 214.0 and 152.0 F g<sup>-1</sup> at scan rates of 10, 25, 50 and 100 mV s<sup>-1</sup>, respectively. Fig. S7d shows the galvanostatic charge/discharge tests of the MoS<sub>2</sub> electrode at various current densities of 1, 2, 4 and 8 A g<sup>-1</sup>. Obviously, the discharge curve can be divided into two sections, a sudden potential drop due to the internal resistance and a slow potential decay due to the Faradic redox reaction, further suggesting

the pseudocapacitive behavior in this system. The specific capacitances are calculated to be 180.4, 168.6, 150.4 and 118.4 F g<sup>-1</sup> at the current densities of 1, 2, 4 and 8 A g<sup>-1</sup>, respectively.

The CV curves of the defect-rich MoS<sub>2</sub> ultrathin nanosheets electrode in 3 M KOH at various scan rates display prominent reversible redox peaks, suggesting the pseudocapacitive properties (Fig. S7e). Additionally, the redox peaks are gradually expanded with increased scan rate. The results are similar with those in LiOH solution. The specific capacitances of the electrode calculated from the CV curves are 390.7, 328.0, 268.0 and 199.3 F g<sup>-1</sup> at scan rates of 10, 25, 50 and 100 mV s<sup>-1</sup>, respectively. Fig. S7f shows the galvanostatic charge/discharge profiles of the MoS<sub>2</sub> electrode with different current densities, where the two section of discharge curve is similar with that in LiOH solution, and the capacitances are 211.2, 184.8, 162.4 and 128.2 F g<sup>-1</sup> at the current densities of 1, 2, 4 and 8 A g<sup>-1</sup>, respectively. The specific capacitance of our defect-rich MoS<sub>2</sub> ultrathin nanosheets electrode is nearly the same as that of the porous tubular C/MoS<sub>2</sub> nanocomposites with 210 F g<sup>-1</sup> at the current density of 1 A g<sup>-1</sup>,<sup>4</sup> and larger than flower-like MoS<sub>2</sub> microspheres with 185 and 166 F g<sup>-1</sup> at the current densities of 1 and 2 A g<sup>-1</sup>.<sup>5</sup>

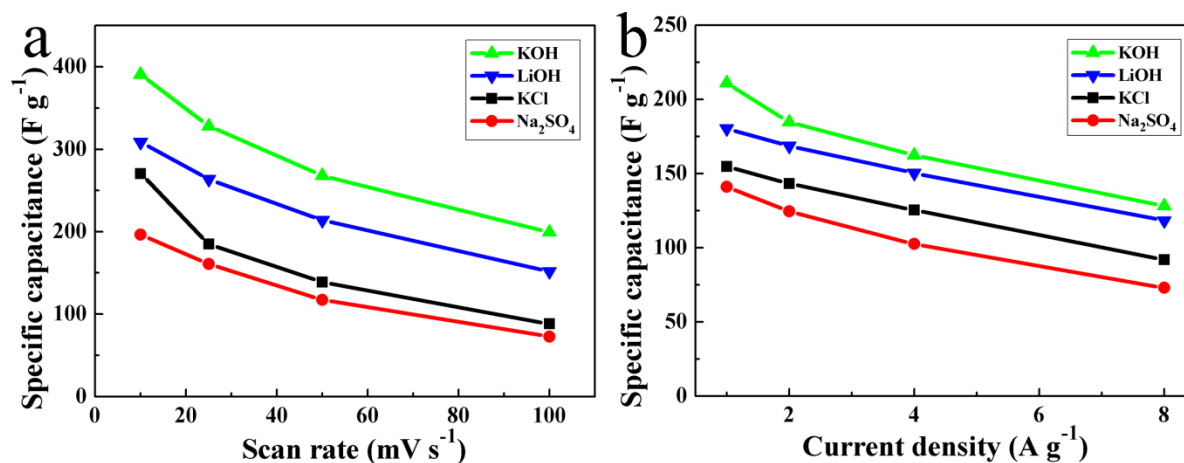


**Fig. S8** The specific capacitances of the defect-rich MoS<sub>2</sub> ultrathin nanosheets electrodes with various electrolytes of KCl, Na<sub>2</sub>SO<sub>4</sub>, LiOH and KOH. (a) at different scan rates; and (b) at different current densities.

The comparison of the specific capacitances of the defect-rich MoS<sub>2</sub> ultrathin nanosheets electrode with various electrolytes of KCl, Na<sub>2</sub>SO<sub>4</sub>, LiOH and KOH at different scan rates and current densities clearly revealed the capacitance of the electrode was dependent on the electrolyte. The high electrical conductivity as well as the ability to adsorb and intercalate various ions of the defect-rich MoS<sub>2</sub> ultrathin nanosheets makes the MoS<sub>2</sub> electrode can be applied in various electrolytes for supercapacitors.

## References

- 1 S. Patil, A. Harle, S. Sathaye and K. Patil, *CrystEngComm*, 2014, **16**, 10845–10855.
- 2 S. Ratha and C. S. Rout, *ACS Appl. Mater. Interfaces* 2013, **5**, 11427–11433.
- 3 K. J. Huang, J. Z. Zhang, G. W. Shi and Y. M. Liu, *Electrochim. Acta*, 2014, **132**, 397–403.
- 4 B. L. Hu, X. Y. Qin, A. M. Asiri, K. A. Alamry, A. O. Al-Youbi and X. P. Sun, *Electrochim. Acta*, 2013, **100**, 24–28.
- 5 L. Ma, L. M. Xu, X. P. Zhou and X. Y. Xu, *Mater. Lett.*, 2014, **132**, 291–294.